processes

MDPI

Article

Role of Biosynthesized Silver Nanoparticles with *Trigonella foenum-graecum* Seeds in Wastewater Treatment

Manal A. Awad [1], Promy Virk [2,*], Awatif A. Hendi [3], Khalid Mustafa Ortashi [4], Najla AlMasoud [5] and Taghrid S. Alomar [5,*]

[1] King Abdullah Institute for Nanotechnology, King Saud University, Riyadh 11451, Saudi Arabia; mawad@ksu.edu.sa
[2] Department of Zoology, King Saud University, Riyadh 11451, Saudi Arabia
[3] Department of Physics, College of Science, Princess Nourah bint Abdulrahman University, Riyadh 11671, Saudi Arabia; aahindi@pnu.edu.sa
[4] Department of Chemical Engineering, King Saud University, Riyadh 11421, Saudi Arabia; ortashi9@ksu.edu.sa
[5] Department of Chemistry, College of Science, Princess Nourah bint Abdulrahman University, P.O. Box 84428, Riyadh 11671, Saudi Arabia; nsalmasoud@pnu.edu.sa
* Correspondence: bvirk@ksu.edu.sa (P.V.); tsalomar@pnu.edu.sa (T.S.A.)

Abstract: As the human population continues to escalate, its requirement for clean water is also increasing. This has resulted in an increased dependency on wastewater effluent to maintain the base flow of urban streams, especially in water-stressed regions. The present study reports the synthesis of AgNPs with green credentials using an aqueous extract of *Trigonella foenum-graecum* seeds. The observance of surface plasmon resonance (SPR) with UV–Vis spectrophotometry confirmed the presence of spherical/oblong particles with a mean diameter of 43.8 nm and low polydispersity index (PDI) of 0.391 measured by transmission electron microscopy (TEM) and DLS (dynamic light scattering) technique, respectively. The elemental map of AgNPs was demonstrated with energy-dispersive spectroscopy (EDS) and the constituent functional groups were identified by the FTIR spectra, which were similar to the bulk seed extract with a slight shift in the pattern. The emission spectrum of nanoparticles was recorded for the excitation wavelength of 349 using fluorescence microscopy and the crystalline structure was assessed using X-ray diffraction. The potential wastewater remedial efficacy of the synthesized AgNPs was evaluated based on the water quality parameters (pH, EC, BOD, COD) of the sewage effluent collected from a local Sewage Treatment Plant (STP). Furthermore, the photo degradative efficacy was investigated using the degradation percentage of Crystal Violet (CV) dye, which was recorded as 94.5% after 20 min. In addition, the antimicrobial activity of the NPs versus bulk seed extract was assessed against two bacterial strains, *Escheria coli* and *Staphylococcus aureus*, using the disc diffusion method. The AgNPs showed a profound modulatory effect on the water quality parameters, coupled with marked antimicrobial and photodegradative activity. Thus, the biogenically synthesized AgNPs offer a prospective potential for use in wastewater remediation strategies.

Keywords: wastewater treatment; sewage effluent; silver nanoparticles; *Trigonella foenum-graecum* seed; green synthesis; photo degradation

Citation: Awad, M.A.; Virk, P.; Hendi, A.A.; Ortashi, K.M.; AlMasoud, N.; Alomar, T.S. Role of Biosynthesized Silver Nanoparticles with *Trigonella foenum-graecum* Seeds in Wastewater Treatment. *Processes* **2023**, *11*, 2394. https://doi.org/10.3390/pr11082394

Academic Editors: George Z. Kyzas and Andrea Petrella

Received: 10 June 2023
Revised: 10 July 2023
Accepted: 3 August 2023
Published: 9 August 2023

1. Introduction

An increase in the human population and subsequent global warming has led to a rapid depletion of water resources on the planet. The demand for urban water has escalated due to rapid development, population increase, and climate change, particularly in the arid and semiarid regions of the world. The water requirements in water-stressed regions are met by urban streams or reservoirs that are increasingly dependent on wastewater from sewage treatment plants (STPs) to maintain the base flows into aquatic habitats [1]. Since

freshwater resources are limited, modern methods of conserving them include the selective use of water resources and the reuse of treated wastewater for a variety of applications [2,3].

Nanotechnology is a promising scientific discipline that has made significant advances in several areas, including wastewater treatment. The primary goal of nanotechnology is to create unique structures with improved electrical, optical, magnetic, conductive, and mechanical capabilities by manipulating matter at the molecular and atomic scales [4]. Heavy metals, organic and inorganic solvents, biological toxins, and pathogens are common pollutants in wastewater that have been shown to be effectively cleaned up by nanomaterials [5,6]. The most extensively investigated nanomaterials in current times for water and wastewater treatment processes include carbon nanotubes (CNTs), metal oxide nanoparticles, zero-valent metal nanoparticles, and nanocomposites [7,8]. In the field of wastewater treatment, silver nanoparticles (AgNPs) and their hybrids are currently gaining impetus [9]. Silver nanoparticles (Ag NPs) exhibit remarkable toxicity to microbes and thus possess potent microbicidal activity against a broad spectrum of microbes, including viruses, bacteria, and fungi [10,11]. Furthermore, their improved adsorption capacities distinguish them as viable alternatives in eliminating contaminants such as the dyes rhodamine, Congo red, and methyl orange commonly found in wastewater bodies [12]. Furthermore, the conventional chemical and physical approaches in synthesis of AgNPs consume time, energy, and capital in addition to the toxic side effects generated with repeated use. Currently, green modes of synthesis, also termed biosynthesis, utilize microbes, fungi and medicinal plants/herbs which are easily available, easy to handle, and provide a wide array of metabolites for the synthesis of AgNPs, as well as being nontoxic and ecofriendly [13–16].

The major focus in biosynthesis has been on the utilization of plant extracts due to their abundant availability and phytochemical profile [17,18]. In order to reduce the silver in silver nitrate, which is employed as a precursor in the biosynthesis of AgNPs, phytocompounds are typically used as alternative reducing or capping agents. Several plant extracts have been used in the past to synthesize AgNPs, including *Papaver somniferum* [19], *Bauhinia variegata* L. [20], *Hevea brasiliensis* [21], *Aloe vera* [22], and *Moringa oliefera* [14], as well as stem extract from the cotton plant *Gossypium hirsutum* and *Portulaca oleracea* leaves [23,24]. The plant *Trigonella foenum-graecum*, also referred to as fenugreek, is a member of the Leguminoseae (Fabaceae) family. The phyto-constituent profile of the seeds and leaves of fenugreek reveal that they are nutrient-dense and packed with vital phytochemicals that provide the herb its therapeutic effects. These include proteins, lipids, alkaloids, flavonoids, fibers, saponins, steroidal saponins, vitamins, and minerals. Additionally, it exhibits antioxidant, antibacterial, anti-diabetic, and anticancer effects [25,26]. For various biomedical and environmental remediation applications, fenugreek seed extract and leaves have been used in several prior studies to biogenically synthesize silver nanoparticles (AgNPs) [27–30].

From this premise, the present study reports a novel biogenic synthesis of AgNPs with *Trigonella foenum-graecum* seeds with further effective nanonization which has received a patent. Furthermore, this study includes an assessment of their potential in wastewater remediation based on photodegradative efficacy, modulatory effect on water quality parameters, and antimicrobial potency.

2. Materials and Methods

2.1. Green Synthesis of Ag Nanoparticles

Trigonella foenum-graecum seeds were purchased from the neighborhood market in Riyadh, Saudi Arabia. Cleansed, dried, and powdered seeds were used. We boiled 10 g of powdered seeds in 100 mL of distilled water (pH 6.10) for 2 min to prepare the aqueous extract. The extract was then filtered through Whatman 40 filter paper, and the filtrate was stored at 4 °C for further use. The silver nanoparticles (AgNPs) (pH 5.32) were then prepared using the aqueous seed extract according to Awad et al. [27] with certain modifications (Figure 1).

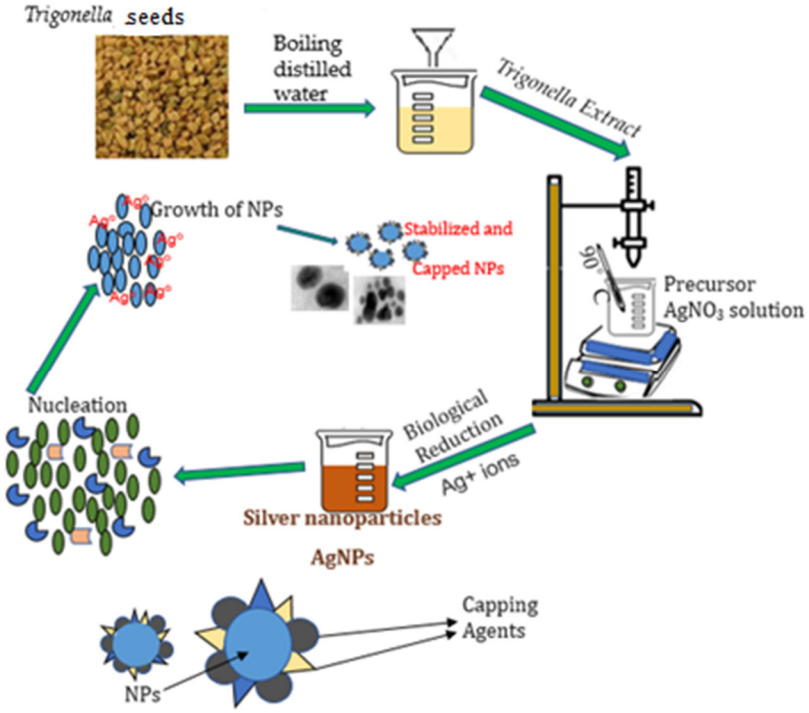

Figure 1. Illustration of the mode of synthesis of the AgNPs using *Trigonella* seed extract.

2.2. Characterization of Synthesized AgNPs

The UV–Vis absorbance using ultraviolet–visible spectroscopy (Perkin Elmer UV–Vis spectrometer, Buckinghamshire, UK) confirmed the reduction of silver ions to silver nanoparticles in the presence of *Trigonella* seed extract. The average particle size of AgNPs was analyzed by Zetasizer, Nano series, HT Laser, ZEN3600 (Molvern Instruments, Malvern, UK). Transmission and Scanning electron microscopy (TEM and SEM) was used to assess the size, shape, and morphologies (JEOL-FE-SEM TEM, Tokyo, Japan), and energy dispersive spectrometer (EDS) analysis was carried out for the detection of elemental silver. Fourier transform infrared (FTIR) spectra in the range of 400–4000 cm^{-1} were recorded using a Perkin-Elmer 100 spectrophotometer [27,31,32].

2.3. Treatment of Sewage Effluent by Synthesized AgNPs

Grab samples of sewage effluent were collected from the Sewage Treatment Plant (STP) at Al-Hahsa City, Saudi Arabia, in plastic barrels. Samples of tap water were collected in polyethylene bottles directly from the laboratory. Three bottles of 3 L capacity were taken in the laboratory; in two bottles, the sewage effluent was added, and in one, the normal tap water was added. About 50 mgL^{-1} of synthesized AgNPs were added to one of the bottles which contained 3 L the sewage effluent. The bottles were then kept aside for 72 h, after which the treated effluent was filtered. Water quality parameters were assessed for the treated effluent, untreated effluent and tap water.

2.4. Antibacterial Activity of Silver Nanoparticles

To assess the microbicidal efficacy of the silver nanoparticles, pure cultures of Gram-positive and Gram-negative bacteria, *Escherichia coli* and *Staphylococcus aureus* were utilized. The disc diffusion method was used to evaluate the antibacterial activity [33]. Plates containing nutrient agar were prepared, sterilized, and solidified. Thereafter, the test bacterial cultures were inoculated onto the plates. The sterile discs were coated with nanoparticle solutions at two doses of 1 and 0.5 gmL^{-1} and then placed in nutritional agar medium, where they were cultured for 24 h at 370 °C. A zone of clearing surrounding the wells, which was measured as the diameter of the inhibition zone, was used to demonstrate

the inhibitory activity of the bulk aqueous extract of Trigonella seeds and the nanoparticles (AgNPs).

2.5. Statistical Analysis

The mean and standard deviation (Mean ± SD) for all parameters relating to water quality are used to express the data. To analyze group differences, a one-way analysis of variance was conducted, followed by a Tukey's test (SPSS 22.0 statistical program, Chicago, IL, USA). The threshold for significance was fixed at $p \leq 0.05$.

3. Results and Discussion

3.1. Synthesis and Characterization of the Nanoparticles

Synthesis of AgNPs through the reduction of silver nitrate by phyto-constituents of aqueous *Trigonella* seed extract was confirmed by an observable change in the color of the solution to brown [32,34].

3.1.1. UV–Vis Spectrophotometry

The observed surface plasmon resonance (SPR) by the UV–Vis spectrophotometry confirmed the formation of AgNPs. A strong and broad surface plasmon resonance (SPR) has been seen in metal nanoparticles between 2 and 100 nm in size. Spherical nanoparticles demonstrate a single SPR band, in agreement with Mie's theory [35,36]. Figure 2 shows the absorption peak of the AgNPs solution corresponds to the SPR obtained in a visible range at 439.29 nm. In line with these results, it has been reported that AgNPs exhibit a distinctive absorption peak at about 400 nm, attributed to SPR. The free electrons of the metal NPs are responsible for the SPR absorption peak attributed to the combined vibration of electrons with the light wave [26]. The refractive index of the surrounding medium, particle size, and adsorbed species on their surfaces affects the position of the SPR absorption peak (kmax) of spherical AgNPs [37,38].

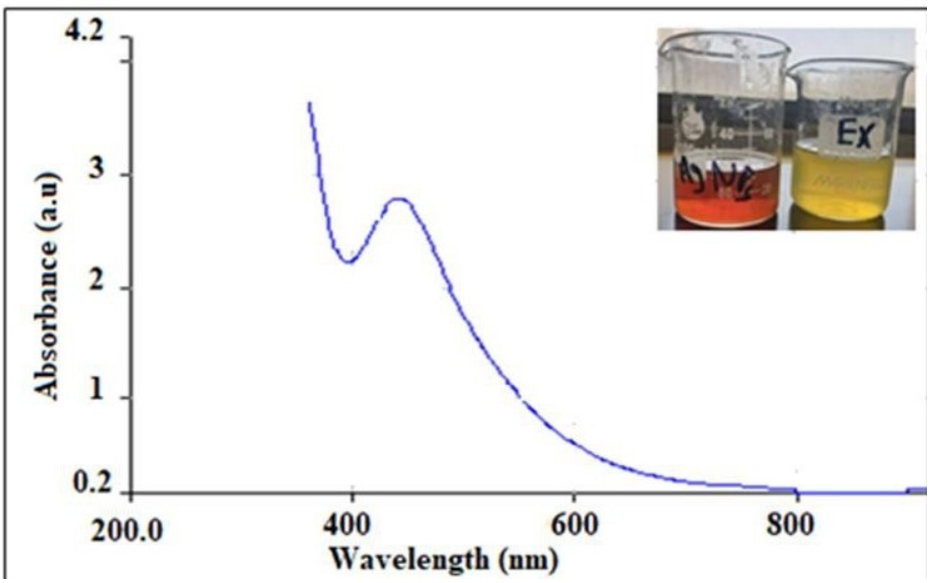

Figure 2. UV–Vis spectrum of the synthesized *Trigonella* AgNPs.

3.1.2. Size and Morphology of Nanoparticles

The particle size distribution by intensity determined using the DLS technique is illustrated in Figure 3. The average hydrodynamic diameter of the prepared AgNPs using *Trigonella* seeds was 43.8 d.nm with an intercept of 0.870 and low polydispersity index (PDI) of 0.391. Similar hydrodynamic radii of AgNPs obtained with DLS in the range of 9–42 nm were reported by Ahani and Khatibzadeh [39]. In comparison to the

TEM measurement of the particle size, the particles were moderately larger in DLS, as it measures the hydrodynamic radius of the particles [40,41].

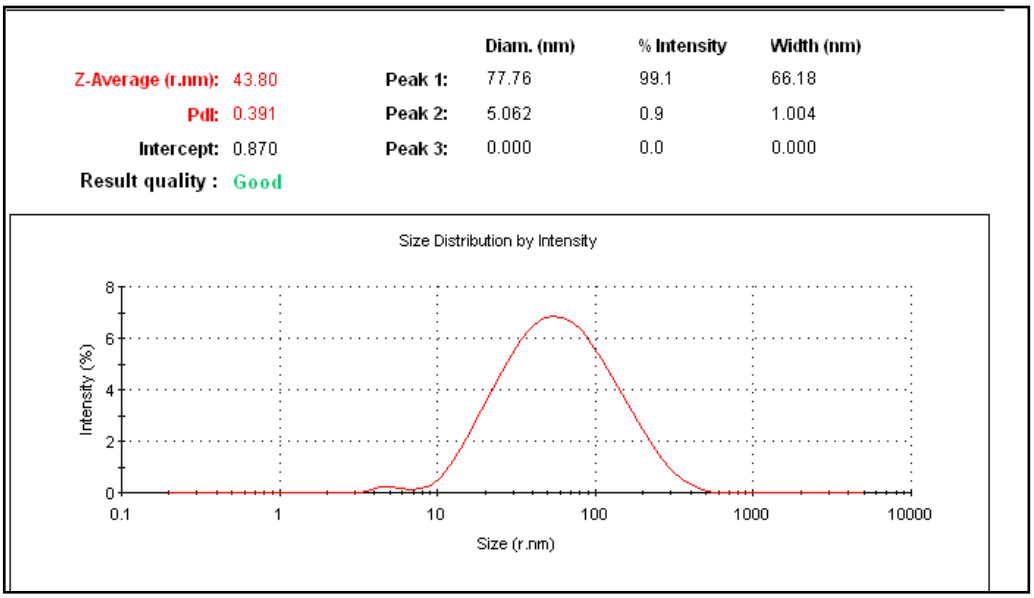

Figure 3. Representative DLS spectrum of synthesized *Trigonella* AgNPs showing the average size of the nanoparticles.

The TEM micrographs illustrated that the synthesized Ag NPs were dispersed without agglomeration. In addition, their morphotype was spherical and oblong, with an average particle size that ranged between 9 and 21 nm (Figure 4). The particle sizes observed in the TEM images are in consensus with a previous study that reported green synthesized Ag NPs with an average size of 20–50 nm [41], and are smaller than those reported by Goyal et al. [32].

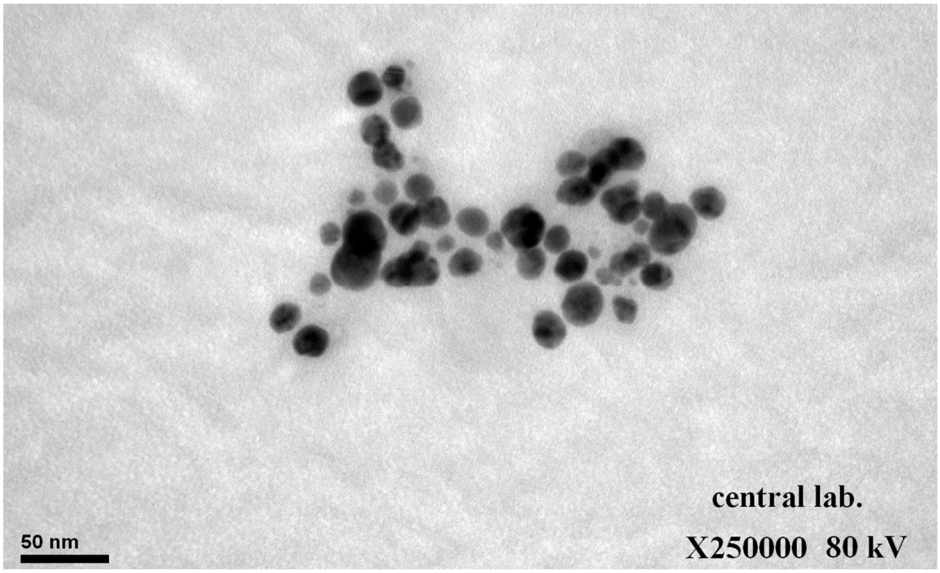

Figure 4. TEM micrograph showing the morphotype of the *Trigonella* AgNPs.

The energy-dispersive spectroscopy (EDS) revealed the elemental map of AgNPs. The silver ions in AgNPs are represented by a prominent peak at 3 keV. AgNPs often show a typical absorption peak at 3 keV because of the surface plasmon resonance. In addition to K and Zn, 87.45% of the Ag was found to be present in AgNPs at 3 keV (Figure 5a,b). The

presence of K and Zn atoms in the aqueous extract of *Trigonella* seeds could possibly be due to the presence of other bioactive components [42,43].

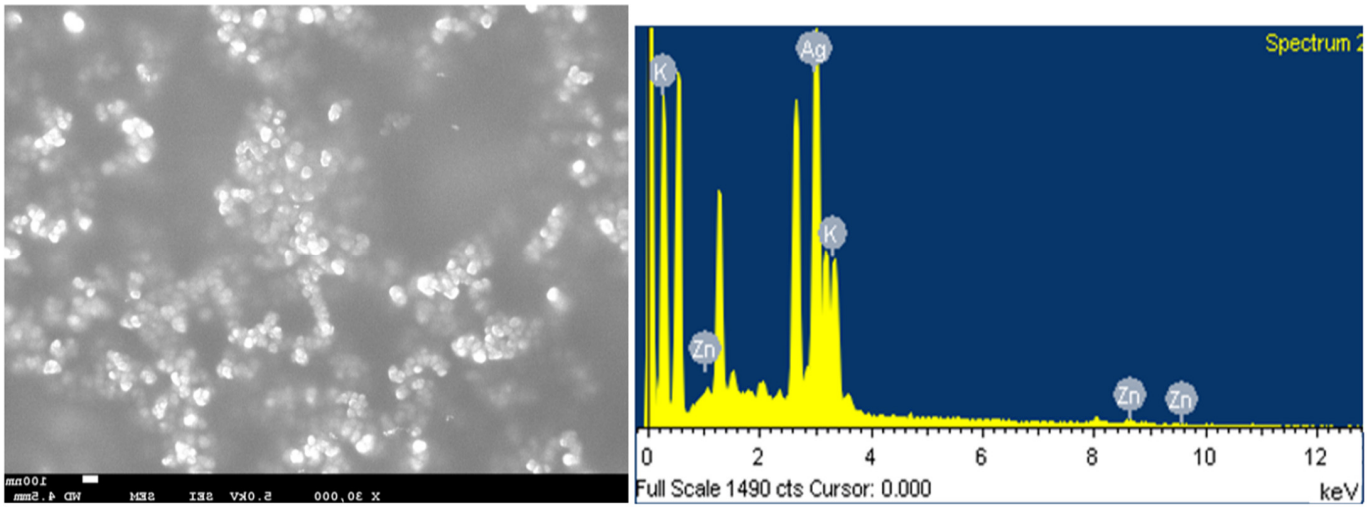

(**a**) (**b**)

Figure 5. (**a**) SEM micrograph of *Trigonella* AgNPs with the (**b**) corresponding EDS spectrum.

3.1.3. FTIR Analysis

FTIR is vital structural tool used to assess the chemical interactions between the metal particles and biomolecules in plant extracts. This gives an insight into the surface chemical composition of the silver nanoparticles along with an identification of the biomolecules that are involved in the capping and stabilization of the metal nanoparticles [44].

The absorption band intensities in the spectra for bulk *Trigonella* seed extract and AgNPs are illustrated in Figure 6. The FTIR spectra of both the bulk *Trigonella* seed extract and AgNPs show different major peaks positioned at 3409.30, 3400.07, 2924.49, 2928.22, 1564.61, 1651.97, 1394.33, 1390.78, 1103.62, 1072.28, 875.30, 835.95, 777.43, 765.98, 613.54, and 615.81 cm^{-1}. The presence of the bio-components from the seed extract in the sample acting as a capping agent for the AgNPs is clearly demonstrated by certain similarities between the spectra, with small marginal shifts in peak positions. Aliphatic primary amines are responsible for the medium N-H stretching that causes the peak at 3400–3409 cm^{-1}. The band at 2924–2928 cm^{-1} is recognized as medium C-H stretching of the alkane group. The peaks at 2129–2195 cm^{-1} correspond to strong C=N=C stretching of the carbodiimide group. The broad peaks at 1564–1651 cm^{-1} correspond to medium N-H bending of the amine group. Peaks between 1072–1103 cm^{-1} are ascribed to strong C-O stretching of secondary alcohol. Peaks below 800 cm^{-1} correspond to strong C=C bending of the alkene group. The alkyl halides band, particularly the C-Cl bond, has a peak in the 628 cm^{-1} range [45]. Therefore, it may be concluded that these biomolecules aid in capping and effectively stabilize the synthesized Ag-NPs [32,44].

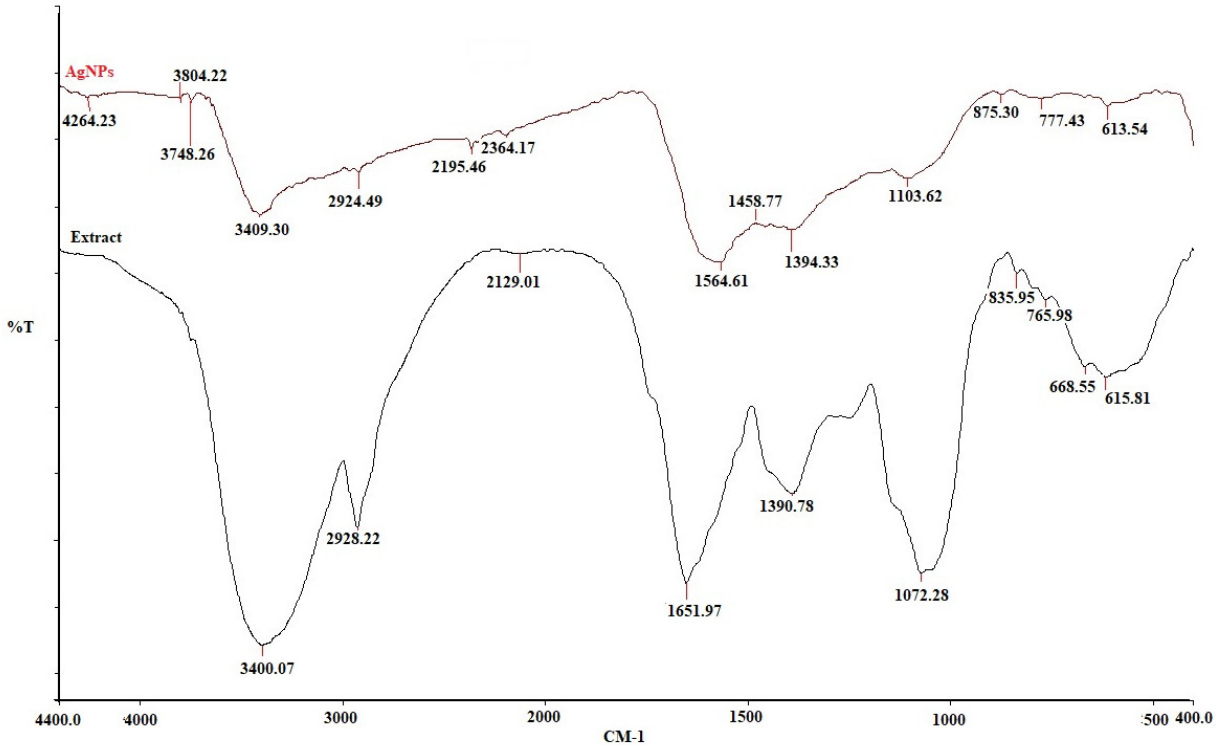

Figure 6. FTIR spectra of *Trigonella* AgNPs and the bulk seed extract.

3.1.4. Fluorescence Spectroscopy

One technique for evaluating the optical characteristics of nanoparticles as photonic materials is the fluorescence (FL) spectrum. The most important criterion for surface plasmon resonance is frequently the collective oscillation of the silver-conducting electrons. AgNPs have a greater visible light resolution than any other known organic or inorganic chromophore. The nature, size, and shape of the surrounding particles in suspension strongly influence surface plasmon resonance [46].

Furthermore, the optical properties and electronic characteristics of the AgNPs were assessed (Figure 7). The synthesis of silver nanoparticles further increases the intensity of emission. Synthesized colloidal AgNPs are dispersed in water, and the fluorescence emission spectrum is recorded for the excitation wavelength at 349 nm. The three stages of the fluorescence phenomenon are photoexcitation of an electron, relaxation of the excited electron, and lastly, fluorescence emission. A shift in the emission fluorescence spectra at 699 nm was detected, and the effect of photoexcitation at a wavelength of 349 nm from states above the Fermi level was assessed. The process of electron phonon and hole phonon scattering was related to the fluorescence shift [45]. The transition of the lowest unoccupied molecular orbital (LUMO) to the highest occupied molecular orbital (HOMO), and the transition from HOMO to LUMO+3 and LUMO+4, were all reported to correspond to the band in UV–Vis spectroscopy. Since LUMO+3/+4's orbital compositions are comparable to those of LUMO, the p-sp transition (ligand-to-metal charge transfer, or LMCT) is likewise the primary cause of the transition. These two bands are hence the result of the sp-sp interband transition. AgNPs exhibit intense red emission in their crystalline state, with a maximum emission wavelength in the fluorescence spectrum [47].

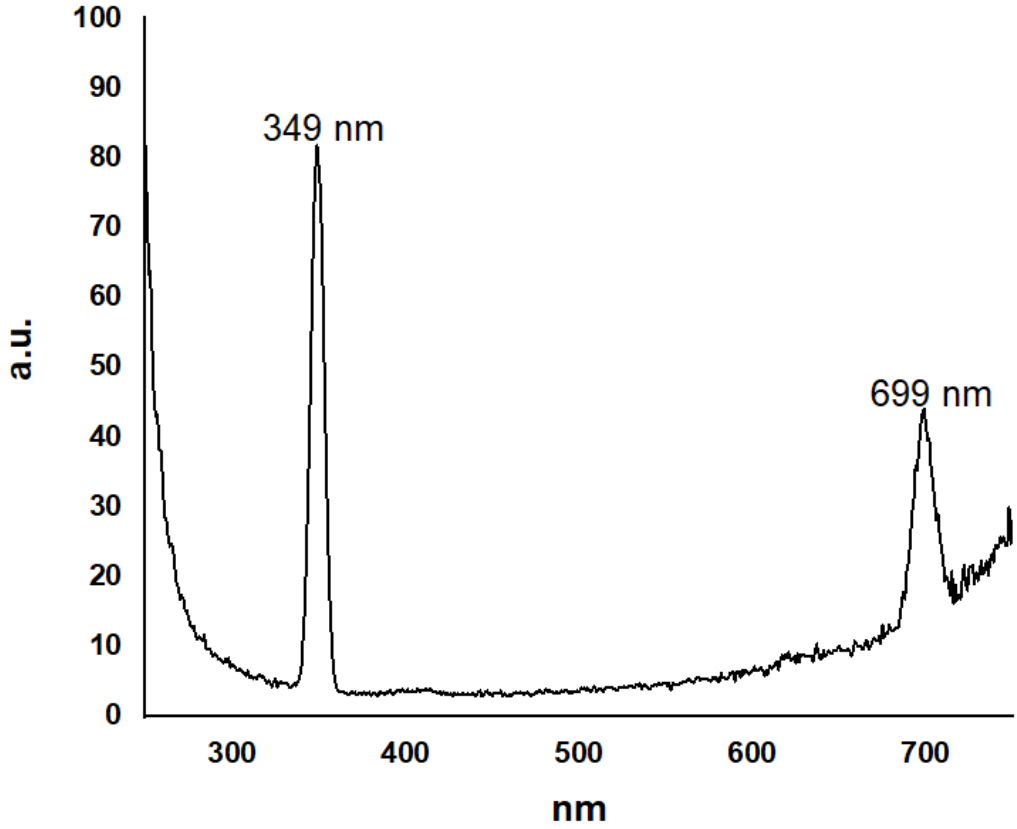

Figure 7. Fluorescence spectrum exhibiting the optical properties and electronic characteristics of the *Trigonella* AgNPs.

3.1.5. X-ray Diffraction Analysis

The Bragg's law, which is based on a wide-angle elastic scattering of X-rays, is the fundamental idea behind the XRD technique. In other words, when exposed to X-rays, the crystal creates a variety of diffraction patterns that show the physicochemical characteristics of the crystal structure. The crystalline nature of AgNPs was investigated and validated in the current work through XRD analysis, as shown in Figure 8. As can be observed, the X-ray diffraction spectrum demonstrated the existence of prominent peaks in the diffraction values that were at 2 theta 38.185° (1 1 1), 44.381° (2 0 0), 64.573° (2 2 0), 77.557° (3 1 1), and 81.715° (2 2 2), along with the corresponding patterns, respectively. This documents and evidences the crystal planes of the face-centered cubic silver structure and crystalline nature (JCPDS COD 9011607) with high purity. Similar patterns for the AgNPs have been also reported in previous studies [48,49].

3.2. Photocatalytic Degradation of Crystal Violet (CV) Dye by AgNPs

The noble metal, silver has the highest potent localized surface plasmon resonance with low optical loss in comparison to other metals. Hot electrons from the silver nanoparticles (Ag NPs) move to the oxygen absorbed on the Ag NPs during localized surface plasmon resonance (LSPR), which causes the oxygen-absorbed Ag nanostructure to become negatively charged. In addition, the heated electrons accelerate the plasmonic Ag NPs' catalytic oxidation reaction [50,51]. As shown in Figure 9, the AgNPs exhibited appreciable degradation of crystal violet dye under UV irradiation. The computed percentage of degradation efficiency was 94.5%.

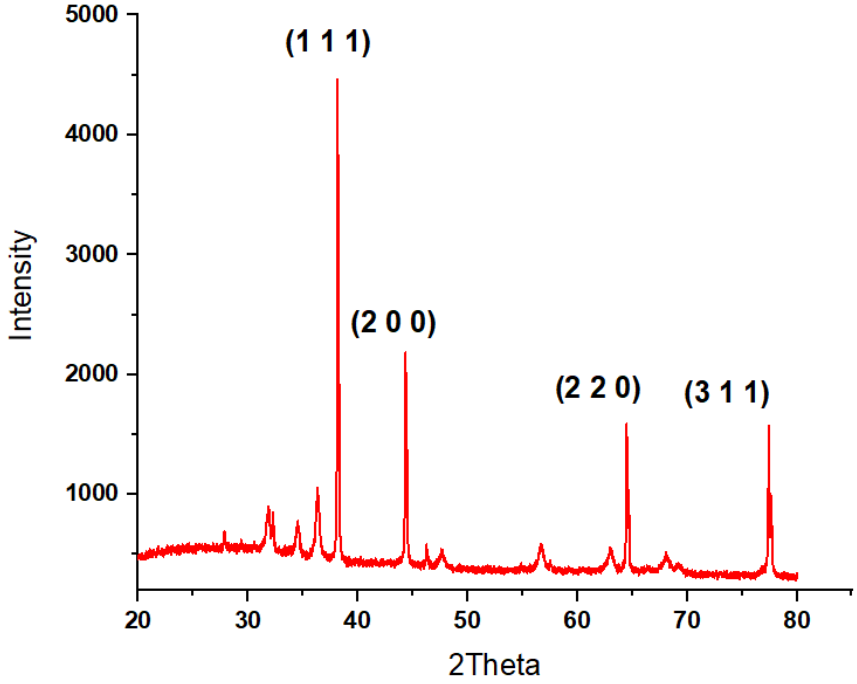

Figure 8. X-ray diffractogram of *Trigonella* AgNPs.

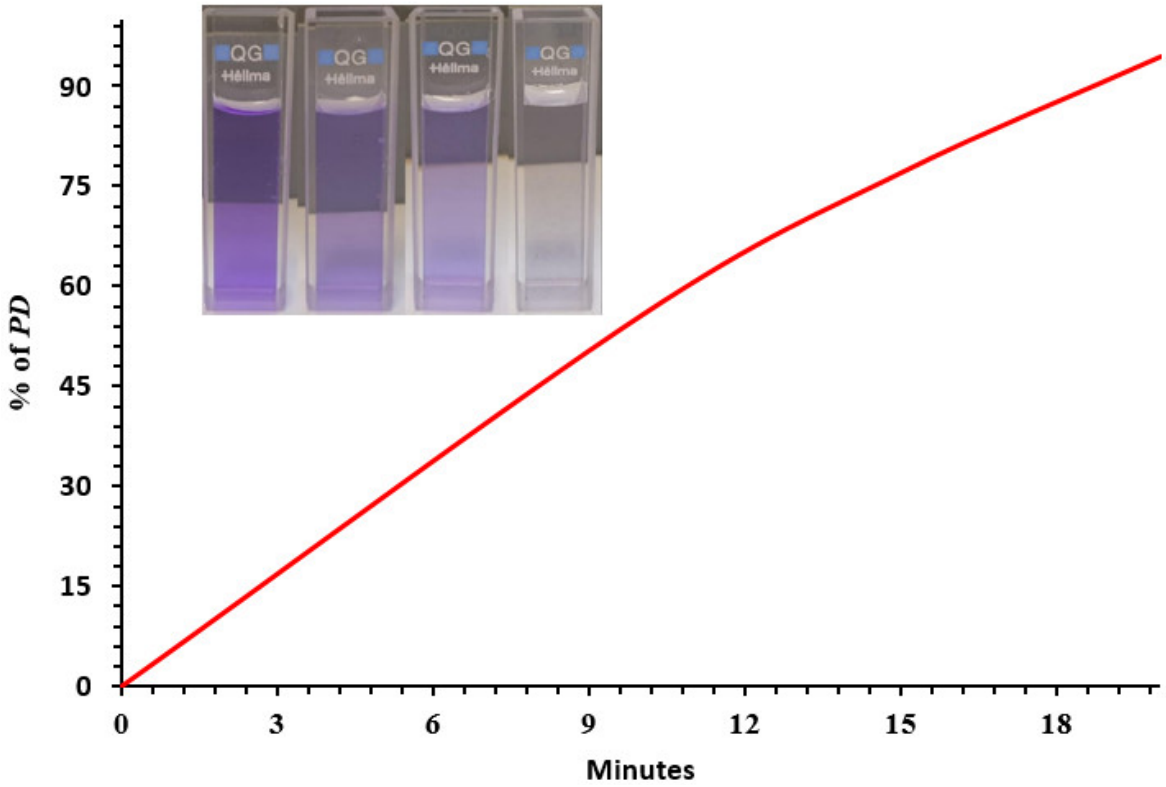

Figure 9. Time-dependent photodegradative percentage of CV dye under UV irradiation by the AgNPs.

Figure 10 presents an illustration of the photocatalytic mechanism of green synthesized AgNPs, and could be summarized as

$$\text{AgNPs} + \textit{Photon} \rightarrow \text{Ag}^{+} + \text{e}^{-}\ \text{electron} \quad (1)$$

$$e^- + O_2 \text{ oxygen} \rightarrow {}^*O_2{}^- \text{ oxygen radicals} \quad (2)$$

$$Ag^+ \text{ silver ions} \rightarrow Ag + \text{hole } (h^+) \quad (3)$$

$$h^+ + H_2O \text{ water / } OH^- \text{ hydroxide ions} \rightarrow {}^*OH \text{ radicals} \quad (4)$$

$$\text{CV dye} + OH^* \rightarrow \text{Decolorization of CV dye} \quad (5)$$

Table 1 provides a comparison of photodegradative efficacy of various plant-based AgNPs to validate the potential of the AgNPs used in the present study.

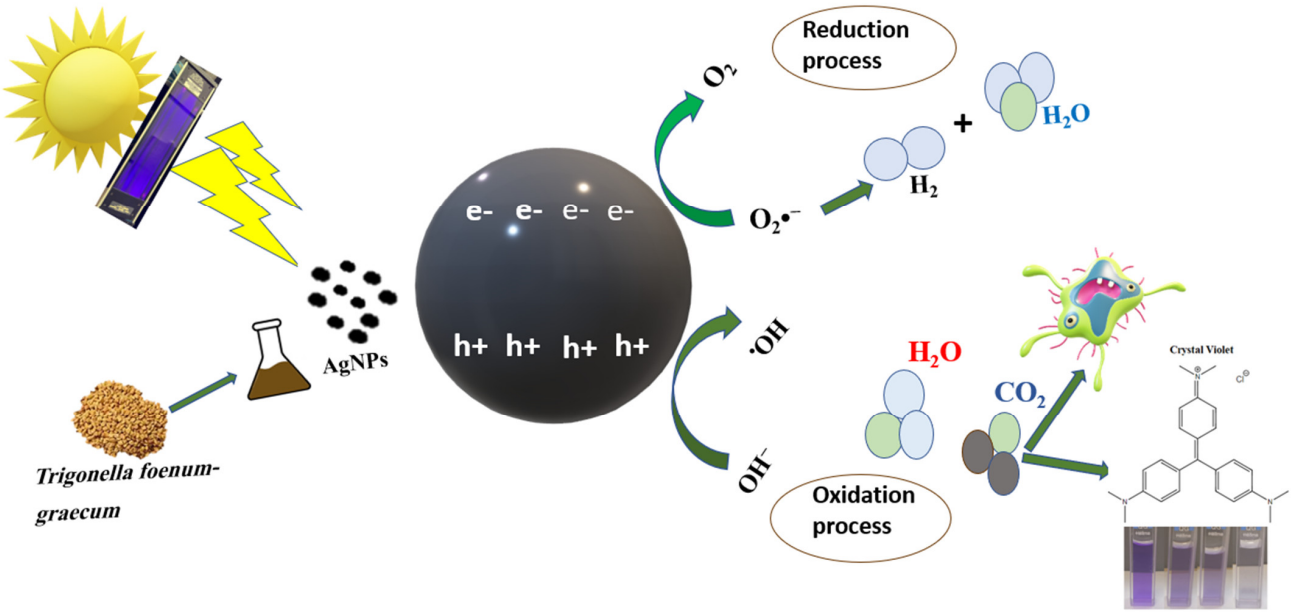

Figure 10. Illustration of the mechanism involved in the photocatalytic degradation of CV dye by AgNPs.

Table 1. Comparative assessment of photodegradative ability of several plant-derived AgNPs reported in the literature with the present study.

Plant	Size (nm)	Illumination Source	Dye/Concentration	Degradation Time/Percentage	Reference
Phaseolus vulgaris (kidney beans)	10–20 nm	Sunlight	RR-141 (50 mL, 20 ppm)	150 min 97%	(Rani et al., 2020) [52]
Trigonella foenum-graecum leaf	5–20 nm	Sunlight	Blue 19 (RB19) and reactive yellow 186 (RY186); respectively	180 min/88% and 86%; respectively	(Singh et al., 2019) [53]
Annona squamosa L.	22 nm	Sunlight	Coomassie brilliant blue(CBB)/5 mL of 1% CBB	Gradually degradation/(10, 20, 30 min)	(Jose et al., 2021) [54]
Trichodesma indicum leaf	35–33 nm	Solar light	Methylene blue (MB) dye/200 mL aqueous solution of MB	82% of MB within 210 min	(Kathiravan et al., 2018) [55]
Cyanthillium cinereum leaf	5–40 nm	Without light irradiation	Methylene blue and fuchsine in the presence of aq.$NaBH_4$/ (0.08×10^{-3} M) of the dyes	Gradual degradation	(Anjana et al., 2021) [56]
Trigonella foenum-graecum seeds	82.53 nm	UV light	Rhodamine B dye/10 μgL^{-1}	(93%) with decoloration after 216 h	(Awad et al., 2021) [27]
Trigonella foenum-graecum seeds	43.80 nm	UV light	Crystal violet/10^{-6} M of dye	94.5% with in 20 min	Present study

3.3. Water Quality Parameters of the Sewage Effluent

Table 2 represents the effect of the synthesized AgNPs on the basic water quality parameters of the sewage effluent. There was a marked alteration in the parameters assessed in terms of pH, EC, inorganic salts, and COD and BOD. It was clearly observed that treatment with AgNPs significantly improved the water quality parameters of the effluent, which is best attributed to the enhanced adsorption activity of the AgNPs coupled with its strong antimicrobial potency [12]. The enhanced adsorption ability of the Ag NPs was evident by the reduction in the EC and inorganic ions. While the decrease in the BOD of the effluent demonstrated a decrease in the microbial count brought about by the AgNPs [10,12,30,57]. Additionally, a significant decrease in the COD values was observed in the effluent on treatment with AgNPs. In consensus with this, recent studies have reported elimination of coliform bacteria and heterotrophic bacteria, with the reduction in the COD of wastewater treatment plants using silver-loaded magnetic nanoparticles [24,58]. The nanoscale size of the nanoparticles provides an increased surface area for an effective adsorption of inorganic/organic matrix in the effluent sample.

Table 2. Effect of *Trigonella* AgNPs on the water quality parameters of sewage effluent.

Parameter	Tap Water	Untreated Sewage Effluent	Sewage Effluent Treated with *Trigonella* Ag-NPs
pH	7.96 ± 0.04160^{a}	8.77 ± 01966^{b}	7.15 ± 0.1101^{c}
EC (ppm)	692.23 ± 4.6801^{a}	1269.36 ± 2.6350^{b}	726.06 ± 3.5232^{c}
SO_4 (ppm)	48.43 ± 0.5132^{a}	166.900 ± 1.3892^{b}	46.67 ± 0.7571^{a}
Cl (ppm)	75.70 ± 0.6083^{a}	552.93 ± 1.6773^{b}	182.93 ± 2.2679^{c}
HCO_3 (ppm)	64.63 ± 0.6806^{a}	57.53 ± 0.6658^{b}	66.03 ± 0.3055^{a}
Mg^{+2} (ppm)	29.73 ± 0.2309^{a}	81.55 ± 0.4500^{b}	47.53 ± 0.5033^{c}
Ca^{+2} (ppm)	82.87 ± 1.0263^{a}	136.03 ± 1.0016^{b}	104.10 ± 0.3605^{c}
COD (mg/L)	0.77 ± 0.0577^{a}	1135.67 ± 8.6217^{b}	805.20 ± 4.9518^{c}
BOD (mg/L)	0.00 ± 0.0000^{a}	49.17 ± 0.9609^{b}	21.57 ± 0.5131^{c}

EC: electrical conductivity; COD: chemical oxygen demand; BOD: biological oxygen demand. Values are expressed as mean ± SD. Different superscripts in a row show significant difference ($p \leq 0.05$).

3.4. Antibacterial Activity of Trigonella/Ag-NPs

Rampant use of antibiotics in recent times, especially during the pandemic, has made the WWTPs act as reservoirs for antibiotic-resistant bacteria, and their potential horizontal gene transfer could have grave implications on human health. Silver nanoparticles have been known for their remarkable antimicrobial activity for decades, being able to combat bacterial infections both in vitro and in vivo. Both Gram-negative and Gram-positive bacteria, as well as strains that are multidrug resistant, are susceptible to AgNPs' antibacterial properties. Above a certain dose, they showed negligible toxicity towards mammalian cells while exhibiting strong toxicity towards bacteria like *E. coli* [10]. Accordingly, the antimicrobial activity of the AgNPs with *Trigonella* seeds in the current study was clearly defined, as the nanoparticles showed a larger diameter of the inhibition zone at two different concentrations than was seen for the bulk *Trigonella* seed extract against two bacterial strains, *E. coli* and *S. aureus* (Table 3). The antibacterial effect on the Gram -positive strain, *S.aureus*, was more pronounced. This is consistent with other studies that found AgNPs made from either *Trigonella* seed or leaf extract to have strong microbicidal activity [27,28,32]. Additionally, AgNPs synthesized by several modes have been extensively documented to have comparable antibacterial properties [23,59]. The electrostatic attraction between the Ag+ ion and the negative charge on the bacterial cell membrane clarifies the antibacterial ability of the Ag-NPs. Thus, the Ag+ ion interferes with bacterial DNA replication and respiration by interacting with enzymes that have thiol groups to form disulfide bridges, permeating the cell membrane, and killing the bacteria [60]. Furthermore, Sabry et al. [61], reported that contact between AgNPs with the bacterial surface leads to an interaction with

the bacterial protein in the cell wall which could interfere with the DNA replication and also trigger the generation of reactive oxygen species which eventually leads to oxidative damage of the bacterial cells. The variability observed in the susceptibility of microbes to the ag-NPs could be attributed to the nature of their cell wall structure, which affects the permeability. The major constituents of the outer membrane of Gram-negative bacteria are lipopolysaccharides that limit the entry of macro/hydrophilic molecules. Conversely, the Gram-positive bacteria have negligible or no lipopolysaccharide content. Furthermore, these bacteria possess multiple peptidoglycan layers and chains of negatively charged glycerin in their cell wall that interacts with the Ag+ ions [32].

Table 3. Diameter of inhibition zone at different concentrations of AgNPs and bulk *Trigonella* seed extract against Gram-positive and -negative bacterial strains.

Bacterial Strain	AgNps		Bulk *Trigonella* Seed Extract
	1 µg/mL	0.5 µg/mL	
Escherichia coli (Gram-negative)	24 mm	20 mm	15 mm
Staphylococcus aureus (Gram-positive)	30 mm	27 mm	14 mm

Currently, water pollution from the sewage of the textile industry in wastewater is one of the major global environmental challenges. Textile wastewater contains a large number of toxic dyes, heavy metals such as mercury, chromium, cadmium, lead, and arsenic, color pigments, and aromatic compounds [29,62]. These toxic chemicals are transported over long distances along with wastewater, and are persistent pollutants in soil and water that have adverse health effects on aquatic fauna, degrade soil fertility, and impair primary production in the aquatic environment with subsequent anoxic conditions [63]. Textile dyes deteriorate the aesthetics of the water bodies, resulting in an increase in BOD and COD, interfering with the food chains, bioaccumulating, and progressing carcinogenicity and mutagenicity [64,65]. In the present study, the *Trigonella*/AgNPs effectively photodegraded the dye, crystal violet, thereby adding to its potential wastewater remediation capacity along with modulation of the water quality parameters of the sewage effluent. Furthermore, its potent anti-microbial activity supported the previous reports on the ability of AgNPs in effectively eliminating over 700 microorganisms found in WWTPs [59]. Thus, synthesis of AgNPs integrating green technology using plant extracts/herbs offers several advantages such as eco-friendliness, biocompatibility, and cost-effectiveness. These distinct properties of AgNPs could prospectively play a vital role in several nanomaterial-based wastewater treatment strategies in modern times.

4. Conclusions

In the current study, a low-cost biogenic synthesis of AgNPs with *Trigonella* seed extract was successfully attempted. The nanoparticles were analytically characterized and their remedial efficacy on wastewater quality and degradative potential of an organic dye showed substantial outcomes that were notable in terms of environmental sustainability. The nanoparticles demonstrated the ability to degrade crystal violet with effective decrease in BOD and COD of the wastewater under optimized conditions. Taken together, the results of the present study show a prospective role of AgNPs using *Trigonella* seeds as an environmentally benign treatment approach for domestic/textile industry wastewater. However, further investigations are imperative to determine the environmental effects of these nanostructures, as well as their viability, via techno-economic feasibility studies.

Author Contributions: Conceptualization, M.A.A. and P.V.; Data curation, A.A.H. and K.M.O.; Formal analysis, K.M.O.; Investigation, M.A.A., A.A.H., N.A. and T.S.A.; Methodology, M.A.A.; Resources, N.A. and T.S.A.; Software, K.M.O.; Validation, A.A.H.; Writing—original draft, M.A.A. and P.V.; Writing—review and editing, P.V. All authors have read and agreed to the published version of the manuscript.

Funding: The authors extend their appreciation to the Deputyship for Research & Innovation, Ministry of Education in Saudi Arabia for funding this research work through the project number RI-44-0191.

Institutional Review Board Statement: Not relevant.

Informed Consent Statement: Not applicable.

Data Availability Statement: Data will be provided on request.

Conflicts of Interest: The authors declare no conflict of interest.

References

1. Luthy, R.G.; Sedlak, D.L.; Plumlee, M.H.; Austin, D.; Resh, V.H. Wastewater-effluent-dominated streams as ecosystem-management tools in a drier climate. *Front. Ecol. Environ.* **2015**, *13*, 477–485. [CrossRef]
2. Kalkan, C.; Yapsakl, K.; Mertoglu, B.; Tufan, D.; Saatci, A. Evaluation of Biological ActivatedCarbon (BAC) process in wastewater treatment secondary effluent for reclamation purposes. *Desalination* **2011**, *265*, 8. [CrossRef]
3. Shittu, K.O.; Ihebunna, O. Purification of simulated waste water using green synthesized silver nanoparticles of Piliostigma thonningii aqueous leave extract. *Adv. Nat. Sci. Nanosci. Nanotechnol.* **2017**, *8*, 045003. [CrossRef]
4. Jain, K.; Patel, A.S.; Pardhi, V.P.; Flora, S.J.S. Nanotechnology in Wastewater Management: A New Paradigm TowardsWastewater Treatment. *Molecules* **2021**, *26*, 1797. [CrossRef]
5. Kumar, S.; Ahlawat, W.; Bhanjana, G.; Heydarifard, S.; Nazhad, M.M.; Dilbaghi, N. Nanotechnology-Based Water Treatment Strategies. *J. Nanosci. Nanotechnol.* **2014**, *14*, 1838–1858. [CrossRef]
6. Ahmed, S.F.; Mofijur, M.; Ahmed, B.; Mehnaz, T.; Mehejabin, F.; Maliat, D.; Hoang, A.T.; Shafiullah, G.M. Nanomaterials as a sustainable choice for treating wastewater. *Environ. Res.* **2022**, *214*, 113807. [CrossRef]
7. Lu, H.; Wang, J.; Stoller, M.; Wang, T.; Bao, Y.; Hao, H. An Overview of Nanomaterials for Water and Wastewater Treatment. *Adv. Mater. Sci. Eng.* **2016**, *2016*, 4964828. [CrossRef]
8. Anjum, M.; Miandad, R.; Waqas, M.; Gehany, F.; Barakat, M.A. Remediation of wastewater using various nano-materials. *Arab. J. Chem.* **2019**, *12*, 4897–4919. [CrossRef]
9. Malik, S.B.; Saggu, J.I.; Gul, A.; Abbasi, B.A.; Iqbal, J.; Waris, S.; Jardan, Y.A.B.; Chalgham, W. Synthesis and Characterization of Silver and Graphene Nanocomposites and Their Antimicrobial and Photocatalytic Potentials. *Molecules* **2022**, *27*, 5184. [CrossRef]
10. Bruna, T.; Maldonado-Bravo, F.; Jara, P.; Caro, N. Silver Nanoparticles and Their Antibacterial Applications. *Int. J. Mol. Sci.* **2021**, *22*, 7202. [CrossRef]
11. Haris, M.; Fatima, N.; Iqbal, J.; Chalgham, W.; Mumtaz, A.S.; El-Sheikh, M.A.; Tavafoghi, M. *Oscillatoria limnetica* Mediated Green Synthesis of Iron Oxide (Fe_2O_3) Nanoparticles and Their Diverse In Vitro Bioactivities. *Molecules* **2023**, *28*, 2091. [CrossRef]
12. Ganguly, K.; Dutta, S.D.; Patel, D.K.; Lim, K. Chapter 18—Silver nanoparticles for wastewater treatment. In *Micro and Nano Technologies, Aquananotechnology*; Abd-Elsalam, K.A., Muhammad Zahid, M., Eds.; Elsevier: Amsterdam, The Netherlands, 2021; pp. 385–401; ISBN 9780128211410. [CrossRef]
13. Galatage, S.T.; Hebalkar, A.S.; Dhobale, S.V.; Mali, O.R.; Kumbhar, P.S.; Nikade, S.V.; Killedar, S.G. Silver Nanoparticles: Properties, Synthesis, Characterization, Applications and Future Trends. In *Silver Micro-Nanoparticles—Properties, Synthesis, Characterization, and Applications*; IntechOpen: Rijeka, Croatia, 2021. [CrossRef]
14. Mohammed, A.B.A.; Mohamed, A.; El-Naggar, N.E.; Mahrous, H.; Nasr, G.M.; Abdella, A.; Ahmed, R.H.; Irmak, S.; Elsayed, M.S.A.; Selim, S.; et al. Antioxidant and Antibacterial Activities of Silver Nanoparticles Biosynthesized by *Moringa oleifera* through Response Surface Methodology. *J. Nanomater.* **2022**, *2022*, 9984308. [CrossRef]
15. Krishnaraj, C.; Jagan, E.G.; Rajasekar, S.; Selvakumar, P.; Kalaichelvan, P.T.; Mohan, N.J.C.S.B.B. Synthesis of silver nanoparticles using *Acalypha indica* leaf extracts and its antibacterial activity against water borne pathogens. *Colloids Surf. B* **2010**, *76*, 50–56.
16. Ullah, Z.; Gul, F.; Iqbal, J.; Abbasi, B.A.; Kanwal, S.; Chalgham, W.; El-Sheikh, M.A.; Diltemiz, S.E.; Mahmood, T. Biogenic Synthesis of Multifunctional Silver Oxide Nanoparticles (Ag_2ONPs) Using *Parieteria alsinaefolia* Delile Aqueous Extract and Assessment of Their Diverse Biological Applications. *Microorganisms* **2023**, *11*, 1069. [CrossRef]
17. Vanlalveni, C.; Lallianrawna, S.; Biswas, A.; Selvaraj, M.; Changmai, B.; Rokhum, S.L. Green synthesis of silver nanoparticles using plant extracts and their antimicrobial activities: A review of recent literature. *RSC Adv.* **2021**, *11*, 2804–2837.
18. Abbasi, B.A.; Iqbal, J.; Yaseen, T.; Zahra, S.A.; Ali, S.; Uddin, S.; Mahmood, T.; Kanwal, S.; El-Serehy, H.A.; Chalgham, W. Exploring Physical Characterization and Different Bio-Applications of *Elaeagnus angustifolia* Orchestrated Nickel Oxide Nanoparticles. *Molecules* **2023**, *28*, 654. [CrossRef]

19. Vijayaraghavan, K.; Kamala Nalini, S.P.; Kannaian, U.P.N.; Dhakshinamoorthy, M. One step green synthesis of silver nano/microparticles using extracts of *Trachyspermum ammi* and *Papaver somniferum*. *Colloids Surf. B* **2012**, *94*, 114–117.
20. Kumar, V.; Yadav, S.K. Synthesis of different-sized silver nanoparticles by simply varying reaction conditions with leaf extracts of *Bauhinia variegata* L. *IET Nanobiotechnology* **2010**, *6*, 1–8. [CrossRef]
21. Guidelli, E.J.; Ramos, A.P.; Zaniquelli, M.E.D.; Baffa, O. Green synthesis of colloidal silver nanoparticles using natural rubber latex extracted from *Hevea brasiliensis*. *Spectrochim. Acta Part A Mol. Biomol. Spectrosc.* **2011**, *82*, 140–145.
22. Tippayawat, P.; Phromviyo, N.; Boueroy, P.; Chompoosor, A. Green synthesis of silver nanoparticles in *Aloe vera* plant extract prepared by a hydrothermal method and their synergistic antibacterial activity. *PeerJ* **2016**, *4*, e2589.
23. Vanti, G.L.; Nargund, V.B.; Basavesha, K.N.; Vanarchi, R.; Kurjogi, M.; Mulla, S.I.; Tubaki, S.; Patil, R.R. Synthesis of *Gossypium hirsutum*-derived silver nanoparticles and their antibacterial efficacy against plant pathogens. *Appl. Organomet. Chem.* **2019**, *33*, e4630. [CrossRef]
24. Saratale, G.D.; Saratale, R.J.; Cho, S.; Ghodake, G.; Bharagava, R.N.; Park, Y.; Mulla, S.I.; Kim, D.; Kadam, A.; Nair, S.; et al. Investigation of photocatalytic degradation of reactive textile dyes by *Portulaca oleracea*-functionalized silver nanocomposites and exploration of their antibacterial and antidiabetic potential. *J. Alloys Compd.* **2020**, *833*, 155083. [CrossRef]
25. Nagulapalli Venkata, K.C.; Swaroop, A.; Bagchi, D.; Bishayee, A. A small plant with big benefits: Fenugreek (*Trigonella foenum-graecum* Linn.) for disease prevention and health promotion. *Mol. Nutr. Food Res.* **2017**, *61*, 1600950. [CrossRef]
26. Basu, T.K.; Srichamroen, A. Chapter—Health Benefits of Fenugreek (*Trigonella foenum-graecum leguminosse*). In *Preedy, Bioactive Foods in Promoting Health*; Watson, R.R., Victor, R., Eds.; Academic Press: Cambridge, MA, USA, 2010; pp. 425–435; ISBN 9780123746283. [CrossRef]
27. Awad, M.A.; Hendi, A.A.; Ortashi, K.M.; Alzahrani, B.; Soliman, D.; Alanazi, A.; Alenazi, W.; Taha, R.M.; Ramadan, R.; El-Tohamy, M.; et al. Biogenic synthesis of silver nanoparticles using Trigonella foenum-graecum seed extract: Characterization, photocatalytic and antibacterial activities. *Sens. Actuators A Phys.* **2021**, *323*, 112670. [CrossRef]
28. Rizwana, H.; Alwhibi, M.S.; Aldarsone, H.A.; Awad, M.A.; Soliman, D.A.; Bhat, R.S. Green synthesis, characterization, and antimicrobial activity of silver nanoparticles prepared using *Trigonella foenum-graecum* L. leaves grown in Saudi Arabia. *Green Process. Synth.* **2021**, *10*, 421–429. [CrossRef]
29. Moond, M.; Singh, S.; Sangwan, S.; Devi, P.; Beniwal, A.; Rani, J.; Kumari, A.; Rani, S. Biosynthesis of Silver Nanoparticles Utilizing Leaf Extract of Trigonella foenum-graecum L. for Catalytic Dyes Degradation and Colorimetric Sensing of Fe^{3+}/Hg^{2+}. *Molecules* **2023**, *28*, 951. [CrossRef]
30. Varghese, R.; Almalki, M.A.; Ilavenil, S.; Rebecca, J.; Choi, K.C. Silver nanopaticles synthesized using the seed extract of *Trigonella foenum-graecum* L. and their antimicrobial mechanism and anticancer properties. *Saudi J. Biol. Sci.* **2019**, *26*, 148–154. [CrossRef]
31. Bhat, R.S.; Alghamdi, J.M.; Aldbass, A.M.; Aljebrin, N.A.; Alangery, A.B.; Soliman, D.A.; Al-Daihan, S. Biochemical and FT-IR profiling of *Tritium aestivum* L. seedling in response to sodium fluoride treatment. *Fluoride* **2022**, *55*, 81–89.
32. Goyal, S.; Gupta, N.; Kumar, A.; Chatterjee, S.; Nimesh, S. Antibacterial, anticancer and antioxidant potential of silver nanoparticles engineered using *Trigonella foenum-graecum* seed extract. *IET Nanobiotechnol.* **2018**, *12*, 526–533. [CrossRef] [PubMed]
33. Balouiri, M.; Sadiki, M.; Ibnsouda, S.K. Methods for in vitro evaluating antimicrobial activity: A review. *J. Pharm. Anal.* **2016**, *6*, 71–79. [CrossRef]
34. Bratovcic, A. Biosynthesis of Green Silver Nanoparticles and Its UV-Vis Characterization. *Int. J. Innov. Sci. Eng. Technol.* **2020**, *7*, 170–176.
35. Xia, Y.; Halas, N.J. Shape-controlled synthesis and surface plasmonic properties of metallic nanostructures. *MRS Bull.* **2005**, *30*, 338–348. [CrossRef]
36. Duan, X.; Liu, N. Magnesium for dynamic nanoplasmonics. *Acc. Chem. Res.* **2019**, *52*, 1979–1989. [CrossRef] [PubMed]
37. Bastús, N.G.; Piella, J.; Puntes, V. Quantifying the sensitivity of multipolar (dipolar, quadrupolar, and octapolar) surface plasmon resonances in silver nanoparticles: The effect of size, composition, and surface coating. *Langmuir* **2015**, *32*, 290–300. [PubMed]
38. El-Desouky, N.; Shoueir, K.; El-Mehasseb, I.; El-Kemary, M. Synthesis of silver nanoparticles using bio valorization coffee waste extract: Photocatalytic flow-rate performance, antibacterial activity, and electrochemical investigation. *Biomass Conv. Bioref.* **2022**, 1–15. [CrossRef]
39. Ahani, M.; Khatibzadeh, M. Green synthesis of silver nanoparticles using gallic acid as reducing and capping agent: Effect of pH and gallic acid concentration on average particle size and stability. *Inorg. Nano-Met. Chem.* **2022**, *52*, 234–240.
40. Ravichandran, V.; Vasanthi, S.; Shalini, S.; Shah, S.A.A.; Tripathyd, M.; Paliwala, N. Green synthesis, characterization, antibacterial, antioxidant and photocatalytic activity of *Parkia speciosa* leaves extract mediated silver nanoparticles. *Results Phys.* **2019**, *15*, 102565. [CrossRef]
41. Meena, R.K.; Chouhan, N. Biosynthesis of silver nanoparticles from plant (fenugreek seeds) reducing method and their optical properties. *Res. J. Recent. Sci.* **2015**, *2277*, 2502.
42. Bilal, M.; Khan, S.; Ali, J.; Ismail, M.; Khan, M.I.; Asiri, A.M.; Khan, S.B. Biosynthesized silver supported catalysts for disinfection of Escherichia coli and organic pollutant from drinking water. *J. Mol. Liq.* **2019**, *281*, 295–306. [CrossRef]
43. Vijayakumar, M.; Priya, K.; Ilavenil, S.; Janani, B.; Vedarethinam, V.; Ramesh, T.; Arasu, M.V.; Al-Dhabi, N.A.; Kim, Y.O.; Kim, H.J. Shrimp shells extracted chitin in silver nanoparticle synthesis: Expanding its prophecy towards anticancer activity in human hepatocellular carcinoma HepG2 cells. *Int. J. Biol. Macromol.* **2020**, *165*, 1402–1409.

44. Ikram, S.A.S. Silver Nanoparticles: One Pot Green Synthesis Using *Terminalia arjuna* Extract for Biological Application. *J. Nanomed. Nanotechnol.* **2015**, *6*, 1000309. [CrossRef]
45. El-Kemary, M.; Zahran, M.; Khalifa, S.A.; El-Seedi, H.R. Spectral characterisation of the silver nanoparticles biosynthesized using *Ambrosia maritima* plant. *Micro Nano Lett.* **2016**, *11*, 311–314. [CrossRef]
46. Kumar, P.P.N.V.; Pammi, S.V.N.; Pratap Kollu, S.K.V.V.; Shameem, U. Green synthesis and characterization of silver nanoparticles using Boerhaavia diffusa plant extract and their antibacterial activity. *Ind. Crops Prod.* **2014**, *52*, 562–566.
47. Hay, P.J.; Wadt, W.R. Ab initio effective core potentials for molecular calculations. Potentials for the transition metal atoms Sc to Hg. *J. Chem. Phys.* **1985**, *82*, 270.
48. Cao, G.; Wang, Y. *Characterization and Properties of Nanomaterials. Nanostructures and Nanomaterials: Synthesis, Properties, and Applications*; Volume 2 of World Scientific series in nanoscience and nanotechnology; World Scientific: Singapore, 2011; pp. 508, 581; ISBN 9814322504/9789814322.
49. Swetha, V.; Lavanya, S.; Sabeena, G.; Pushpalaksmi, E.; Jenson, S.J.; Annadurai, G. Synthesis and characterization of silver nanoparticles from *Ashyranthus aspera* extract for antimicrobial activity studies. *J. Appl. Sci. Environ. Manag.* **2020**, *24*, 1161–1167.
50. Ma, Y.; Tao, L.; Bai, S.; Hu, A. Green Synthesis of Ag Nanoparticles for Plasmon-Assisted Photocatalytic Degradation of Methylene Blue. *Catalysts* **2021**, *11*, 1499.
51. Lee, S.H.; Jo, J.S.; Park, J.H.; Lee, S.W.; Jang, J.W. A hot-electron-triggered catalytic oxidation reaction of plasmonic silver nanoparticles evidenced by surface potential mapping. *J. Mater. Chem. A* **2018**, *6*, 20939–20946. [CrossRef]
52. Rani, P.; Kumar, V.; Singh, P.P.; Matharu, A.S.; Zhang, W.; Kim, K.H.; Rawat, M. Highly stable AgNPs prepared via a novel green approach for catalytic and photocatalytic removal of biological and non-biological pollutants. *Environ. Int.* **2020**, *143*, 105924.
53. Singh, J.; Kumar, V.; Jolly, S.S.; Kim, K.H.; Rawat, M.; Kukkar, D.; Tsang, Y.F. Biogenic synthesis of silver nanoparticles and its photocatalytic applications for removal of organic pollutants in water. *J. Ind. Eng. Chem.* **2019**, *80*, 247–257. [CrossRef]
54. Jose, V.; Raphel, L.; Aiswariya, K.S.; Mathew, P. Green synthesis of silver nanoparticles using Annona squamosa L. seed extract: Characterization, photocatalytic and biological activity assay. *Bioprocess. Biosyst. Eng.* **2021**, *44*, 1819–1829.
55. Kathiravan, V. Green synthesis of silver nanoparticles using different volumes of *Trichodesma indicum* leaf extract and their antibacterial and photocatalytic activities. *Res. Chem. Intermed.* **2018**, *44*, 4999–5012. [CrossRef]
56. Anjana, V.N.; Joseph, M.; Francis, S.; Joseph, A.; Koshy, E.P.; Mathew, B. Microwave assisted green synthesis of silver nanoparticles for optical, catalytic, biological and electrochemical applications. *Artif. Cells Nanomed. Biotechnol.* **2021**, *49*, 438–449. [CrossRef] [PubMed]
57. Perez, M. The Effects of Silver Nanoparticles on Wastewater Treatment and Escherichia Coli Growth. Bachelor's Thesis, Florida State University, Tallahassee, FL, USA, 2012.
58. Najafpoor, A.; Norouzian-Ostad, R.; Alidadi, H.; Rohani-Bastami, T.; Davoudi, M.; Barjasteh-Askari, F.; Zanganeh, J. Effect of magnetic nanoparticles and silver-loaded magnetic nanoparticles on advanced wastewater treatment and disinfection. *J. Mol. Liq.* **2020**, *303*, 112640. [CrossRef]
59. Epelle, E.I.; Okoye, P.U.; Roddy, S.; Gunes, B.; Okolie, J.A. Advances in the Applications of Nanomaterials for Wastewater Treatment. *Environments* **2022**, *9*, 141. [CrossRef]
60. Li, H.; Gao, Y.; Li, C.; Ma, G.; Shang, Y.; Sun, Y. A comparative study of the antibacterial mechanisms of silver ion and silver nanoparticles by Fourier transform infrared spectroscopy. *Vib. Spectrosc.* **2016**, *85*, 112–121. [CrossRef]
61. Sabry, N.; Tolba, S.; Kh, F.; Abdel-Gawad, F.; Bassem, S.; Hossam, F.; El-Taweel, G.E.; Okasha, A.; Ibrahim, M. Interaction between nano silver and bacteria: Modeling approach. *Biointerface Res. Appl. Chem.* **2018**, *8*, 3570–3574.
62. Singha, K.; Pandit, P.; Maity, S.; Sharma, S.R. Harmful environmental effects for textile chemical dyeing practice. In *Green Chemistry for Sustainable Textiles*; Woodhead Publishing: Cambridge, UK, 2021; pp. 153–164.
63. Dutta, S.; Bhattacharjee, J. A comparative study between physicochemical and biological methods for effective removal of textile dye from wastewater. In *Development in Wastewater Treatment Research and Processes*; Elsevier: Amsterdam, The Netherlands, 2022; pp. 1–2.
64. Patil, R.; Zahid, M.; Govindwar, S.; Khandare, R.; Vyavahare, G.; Gurav, R.; Desai, N.; Pandit, S.; Jadhav, J. Constructed wetland: A promising technology for the treatment of hazardous textile dyes and effluent. In *Development in Wastewater Treatment Research and Processes*; Elsevier: Amsterdam, The Netherlands, 2022; pp. 173–198.
65. Al-Tohamy, R.; Ali, S.S.; Li, F.; Okasha, K.M.; Mahmoud, Y.A.G.; Elsamahy, T.; Jiao, H.; Fu, Y.; Sun, J. A critical review on the treatment of dye-containing wastewater: Ecotoxicological and health concerns of textile dyes and possible remediation approaches for environmental safety. *Ecotoxicol. Environ. Saf.* **2022**, *231*, 13160. [CrossRef]